Data Repository Item 1. Analytical methods and data filtering

This supplementary file details sample preparation and analytical methods and should be cited as the paper it accompanies:

Attia, S., Cottle, J.M., and Paterson, S.R., 2020, Erupted zircon record of continental crust formation during mantle driven arc flare-ups: Geology, v. 48, p. 446–451, https://doi.org/10.1130/G46991.1

WHOLE-ROCK GEOCHEMISTRY

Whole-rock major and trace element compositions for 41 of 42 rock samples were analyzed by XRF and ICP-MS at Activation Laboratories in Ancaster, Ontario or by XRF at Pomona College followed by LA-ICP-MS at the Texas Tech University Geosciences Department GeoAnalytical Laboratory. Only sample HLA-47-B was not analyzed for corresponding whole-rock geochemistry.

X-Ray Fluorescence (XRF)

The following methodology is identical to that of Lackey et al. (2012), adapted from Johnson et al. (1999). Samples were prepared in a jaw crusher and powdered in a Rocklabs® Tungsten Carbide head and mill. Sample material was combined with flux (dilithium tetraborate) at a 2:1 ratio (3.5:7 g) and then fused into a glass bead in a graphite crucible, at furnace temperature of 1000°C for 10 minutes. After cooling, the glass beads are crushed, powdered and fused again under the same conditions. Cooled beads were polished on diamond laps before analysis with a 3.0 kw Panalytical Axios wavelength dispersive XRF spectrometer that measures major, minor, and 18 trace elements (SiO2, TiO2, Al2O3, Fe2O3, MnO, MgO, CaO, Na2O, K2O, P2O5, Ba, Ce, Cr, Cu, Ga, La, Nb, Ni, Pb, Rb, Sc, Sr, Th, U, V, Y, Zn, Zr, Pr, Nd, Hf). **Laser Ablation Inductively Coupled Plasma Mass Spectrometry (LA-ICP-MS)**

Polished thin sections were prepared from beads used in previous XRF analyses and analyzed by LA-ICP-MS for trace elements (Sc, V, Ga, Rb, Sr, Y, Zr, Nb, Ba, REE, Hf, Ta, Pb, Th, U) on an Agilent 7500CS ICP-MS and using a dual volume NRW213 nm solid-state laser. The spot diameter was 80 μm, with a pulse rate of 10 Hz and fluence of 11-9 J/cm2. The analysis consists of a background signal of 25 s followed by 60 s of sample ablation. Three spots were analyzed per sample and averaged. USGS standard GSD was analyzed after every two samples (6 spots) and USGS standard BHVO was analyzed a minimum of four times per day to document instrument consistency over time. Data were reduced and normalized using USGS GSD as the calibration standard and CaO as the internal standard. For consistency and to avoid inclusions and spurious signals from fractures only measurements with flat, even signals >10 s long were included in the dataset.

Inductively Coupled Plasma Mass Spectrometry (ICP-MS)

The following information is provided from the Activation Laboratories website. Samples were prepared following the protocol under the RX1 package. This includes crushing (< 7 kg) up to 90% passing 10 mesh, riffle split (250 g) and pulverize (mild steel) to 95% passing 105μ included cleaner sand. The "4Lithoresearch" package is a combination of 4B (major, minor elements) and 4B2 (trace elements).

4B: Samples are prepared and analyzed in a batch system. Each batch contains a method reagent blank, certified reference material and 17% replicates. Samples are mixed with a flux of lithium metaborate and lithium tetraborate and fused in an induction furnace. The molten melt is immediately poured into a solution of 5% nitric acid containing an internal standard and mixed continuously until completely dissolved (~30 minutes). The samples are run for major oxides and selected trace elements (Code 4B) on a combination simultaneous/sequential Thermo Jarrell-Ash

ENVIRO II ICP or a Varian Vista 735 ICP. Calibration is performed using 7 prepared USGS and CANMET certified reference materials. One of the 7 standards is used during the analysis for every group of ten samples.

4B2: Samples fused under code 4B2 are diluted and analyzed by Perkin Elmer Sciex ELAN 6000, 6100 or 9000 ICP/MS. Three blanks and five controls (three before the sample group and two after) are analyzed per group of samples. Duplicates are fused and analyzed every 15 samples. The instrument is recalibrated every 40 samples.

ZIRCON ANALYSES

Sample Preparation

Zircon crystals were extracted from samples by traditional methods of crushing and grinding, followed by separation with a Wilfley table, heavy liquids, and a Frantz magnetic separator. Samples were processed such that all zircons are retained in the final heavy mineral fraction. A split of these grains (generally up to 50 grains) were selected from the grains available and incorporated into a 1" epoxy. The mounts are sanded down to a depth of ~20 microns, polished, imaged, and cleaned prior to isotopic analysis.

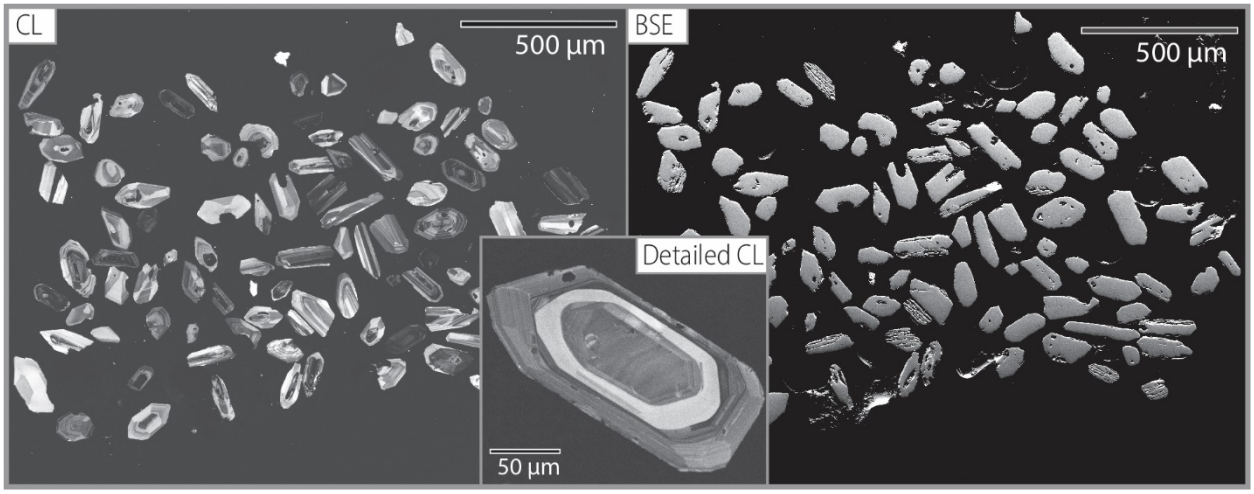

Figure DR1. Examples of zircon SEM imagery.

Scanning Electron Microscopy (SEM)

To guide zircon analysis laser spot selection and placement, zircons on polished epoxy mounts were imaged by Backscattered Electron Microscopy (BSE) and Cathodoluminescence Imaging (CL) at the University of California, Santa Barbara (UCSB) SEM facility.

Laser Ablation Split-Stream Inductively Coupled Mass Spectrometry (LASS) U-Pb Age and Trace Element Analyses

Zircon U-Pb age and trace element (TE) analyses were measured by LASS-ICP-MS over three years (2016, 2017, and 2018) at the University of California, Santa Barbara LASS lab. LASS spot locations were selected with reference to BSE and CL imagery to avoid inclusions or analyses across internal zonation domains. ~40 analyses were typically performed per sample. Up to 5 grains per sample with distinct core and rim zonation apparent in CL were selected for core-rim analyses. The LASS U-Pb age and TE methodology used in this study follows the methodology of Poletti et al. (2016), from which the below text was adapted with minor modification.

The LASS-ICP-MS system combines a Photon Machines 193 nm ArF Excimer laser and Hel-Ex ablation cell with a Nu Instruments HR Plasma high-resolution MC-ICP-MS system for collecting U-Pb data and an Agilent 7700S quadrupole Q-ICP-MS system for collecting major and trace element data. Methods used in this study follow those outlined by Cottle et al. (2012, 2013), Kylander-Clark et al. (2013) and McKinney et al. (2015), except that trace elements were measured via Q-ICP-MS (method outlined below). Laser run conditions used are as follows: 25 μm spot size, 3-4 mJ laser power at 100%, and laser pulse frequency 4 Hz. Before each ablation period, the laser was fired twice to remove contamination from the surface of the analyte, followed by an 8s delay to permit sample washout.

Masses ^{204}Pb + Hg, ^{206}Pb, ^{207}Pb, and ^{208}Pb were measured on ion counters, and ^{232}Th and ^{238}U were measured on Faraday detectors. Every set of eight sample analyses was bracketed by analyses of a primary and a secondary natural reference material. '91500' zircon (Wiedenbeck et al., 1995, 2004) was used as a primary reference material for mass bias and fractionation. 'GJ-1' (Jackson et al., 2004) and 'Plešovice' (Sláma et al., 2008) zircon were used as secondary reference materials to assess data accuracy. Raw U-Pb and trace element data were reduced using Iolite v2.5 (Paton et al., 2011) to correct for instrument drift, laser-ablation-induced down-hole elemental fractionation, plasma-induced elemental fractionation, and instrumental mass bias. Secondary reference materials were used to monitor accuracy and internal reproducibility from run to run, and between analytical sessions. External uncertainty was added to sample isotopic ratios in quadrature and was assigned based on the additional uncertainty needed to produce an MSWD ~1 in a population (n>9) of secondary reference material analyses from the same analytical session. ^{206}Pb/^{238}U typically required the addition of ~1-1.5% external uncertainty. ^{207}Pb/^{206}Pb measurements usually required addition of <1% uncertainty. However, long-term ^{207}Pb/^{206}Pb reproducibility for this laboratory and setup is reported to be 1.5-2% (e.g. Kylander-Clark et al., 2013; Spencer et al., 2013); thus, 1.5% external uncertainty has been added to all ^{207}Pb/^{206}Pb ratios to account for long-term accuracy.

Trace elements of interest were measured in zircon through LASS-ICP-MS simultaneously with U-Pb data. Thus, laser settings, ablation periods, and washout times used for trace element measurement were therefore identical to those described above. The Q-ICP-MS system is equipped with a second Edwards E2M 18 rotary interface pump, increasing sensitivity by about two-fold for elements heavier than Mg. The Q-ICP-MS system was tuned such that ThO+ and CeO+ were less than ~0.5%, and doubly charged ions less than 2%. Dwell time for

elements of stoichiometric abundance (e.g. Zr and Si) was 5 ms. A dwell time of 10 ms was used for trace elements with expected abundances of 10000-1000 ppm (e.g. Hf). For trace elements with expected abundances of ~1000 ppm or less, or those that are generally used for geothermometry (e.g. Ti), dwell time was set to 20 ms. Sweep time was ~0.8 s. Analog detection mode was used for elements of stoichiometric abundance; pulse-counting mode was used for most elements and allowed to switch to analog mode automatically.

'GJ1' zircon was used as the primary reference material for most trace elements in zircon samples [see Liu et al. (2010) for trace element reference values]. '91500' zircon was used as the primary reference material for Si and P because of the lack of 'accepted' values for these elements in 'GJ1' zircon. Trace element reference values used for '91500' are from the GeoReM database, application version 18 (October 2009; http://georem.mpch-mainz.gwdg.de/; Jochum et al., 2005). Secondary trace element reference materials used are the same as the primary U-Pb reference materials. Trace element data were reduced using the 'trace elements' data reduction scheme in Iolite v2.5 (Paton et al., 2011) with the 'semi-quantitative' standardization method. These standardization schemes reproduced values in the secondary reference materials to within 10% or less for most trace elements.

Nine LASS analyses were rejected during data reduction and are excluded from further consideration. For spot analyses younger than 1000 Ma, $^{206}Pb/^{238}U$ ages were interpreted as the best age. Due to an instrumentation issue during LASS U-Pb age and TE analyses in 2018, analyses younger than 1000 Ma conducted in 2018 were assigned the $^{207}Pb/^{235}U$ age. Analyses older than 1000 Ma were assigned the $^{207}Pb/^{206}Pb$ ages.

Lu-Hf Isotopic Analyses

The Lu-Hf isotopic analysis methodology laid out below is also adapted with minor modification from Poletti et al. (2016). Following LASS analyses, a subset of 868 grains were selected for subsequent Lu-Hf isotopic analyses. The subset was selected to focus on grains with reliable age analyses. Laser ablation spot locations for Lu-Hf isotopes, larger than LASS spot sizes, were chosen to avoid analyzing across distinct internal zircon zonation identified in CL and analyze the same domains as LASS spots wherever possible. Ablation spots were placed over the original U-Pb analysis spots to obtain Hf compositions that correspond to the measured U-Pb date of the zircon.

Lu-Hf isotopes in zircon were measured in situ by LA-MC-ICP-MS at UCSB. Methods used in this study are similar to those used by Hagen-Peter et al. (2015) and are summarized here. A laser spot size of 50 μm, 4 mJ laser energy at 100%, and a pulse rate of 10 Hz were used to ablate samples for 50 s, with a 30 s delay between analyses to allow washout. Masses 171-180 were measured on 10 Faraday cups with 1 a.m.u. spacing.

Data were reduced using Iolite v2.5 (Paton et al., 2011). Natural ratios of $^{176}Yb/^{173}Yb$=0.786847 (Thirlwall and Anczkiewicz, 2004) and $^{176}Lu/^{175}Lu$=0.02656 (Chu et al., 2002) were used to subtract isobaric interferences of ^{176}Yb and ^{176}Lu on ^{176}Hf. The Yb mass bias factor was calculated using a natural $^{173}Yb/^{171}Yb$ ratio of 1.123575 (Thirlwall and Anczkiewicz, 2004) and was used to correct for both Yb and Lu mass bias. A natural $^{179}Hf/Hf$ ratio of 0.7325 (Patchett and Tatsumoto, 1980, 1981) was used to calculate the Hf mass bias factor.

To assess accuracy and precision, synthetic reference material zircons ‘MUNZirc1’ and ‘MUNZirc3’ ($^{176}Hf/^{177}Hf$=0.282135±7; Fisher et al., 2011), as well as natural reference material zircons ‘91500’ ($^{176}Hf/^{177}Hf$=0.282308±6; Blichert-Toft, 2008), ‘GJ-1’ ($^{176}Hf/^{177}Hf$=0.282000±5; Morel et al., 2008), ‘Plešovice’ ($^{176}Hf/^{177}Hf$=0.282482±13; Sláma et al., 2008), and ‘Mud Tank’

($^{176}Hf/^{177}Hf$=0.282507±6; Woodhead and Hergt, 2005) were analyzed between every 5-10 sample analyses. The weighted mean corrected $^{176}Hf/^{177}$ Hf values (±2SD) obtained for the secondary reference materials were 0.282136 (n=7) for MUNZirc1, 0.282139 (n=29) for MUNZirc3, 0.282298 (n=22) for 91500, 0.282001 (n=30) for GJ-1, 0.282476 (n=49) for Plešovice, and 0.282422 (n=43) for Mud Tank.

Six analyses were rejected during reduction and are excluded from further consideration. Age corrections for initial Lu-Hf isotopic compositions were carried out with both individual zircon grain U-Pb ages and interpreted sample rock ages. Epsilon Hf was calculated using $^{176}Hf/^{177}Hf$=0.282785 and $^{176}Lu/^{177}Hf$=0.0336 for the chondritic uniform reservoir following Bouvier et al. (2008) and $^{176}Lu = 1{\cdot}867 \times 10^{-11}$ a^{-1} (Scherer et al., 2001, 2003; Söderlund et al., 2004). Uncertainties in corrected $^{176}Hf/^{177}Hf$ ratios were propagated into the εHf initial values; uncertainties in $^{176}Lu/^{177}Hf$ have negligible effect.

Zircon Data Filtering and Interpretation

Reduced zircon data were filtered prior to plotting zircon grain U-Pb ages and calculation of sample rock ages (Fig. 1B of the accompanying paper) with the following criteria: a) Th/U<0.1, to exclude a very small number of possibly metamorphic zircons (REF); b) U>1000 ppm, to exclude analyses more likely to be influenced by radiation damage to crystal lattice; c) analyses older than 500 Ma with greater than 20% discordance or 10% reverse discordance were filtered out to exclude effects of Pb-loss or other disturbances of isotopic ratios; and d) analyses younger than 500 Ma were excluded if the 2-sigma error ellipse did not intersect the concordia line. Interpreted rock ages were calculated as weighted mean ages with 95% confidence errors using Isoplot 3.75 (Ludwig, 2012).

Eight samples did not yield enough reliable analyses to estimate rock ages. IMP samples exhibited contamination with few reliable Mesozoic ages. We assign an age of ~145 Ma to two Iron Mountain pendant samples, collected from a volcanic homocline with overlying Cretaceous strata (Ardill et al., 2018) and interpreted to post-date tilting associated with the Late Jurassic Nevadan orogeny (Tobisch et al., 1989), with a Jura-Cretaceous youngest age population.

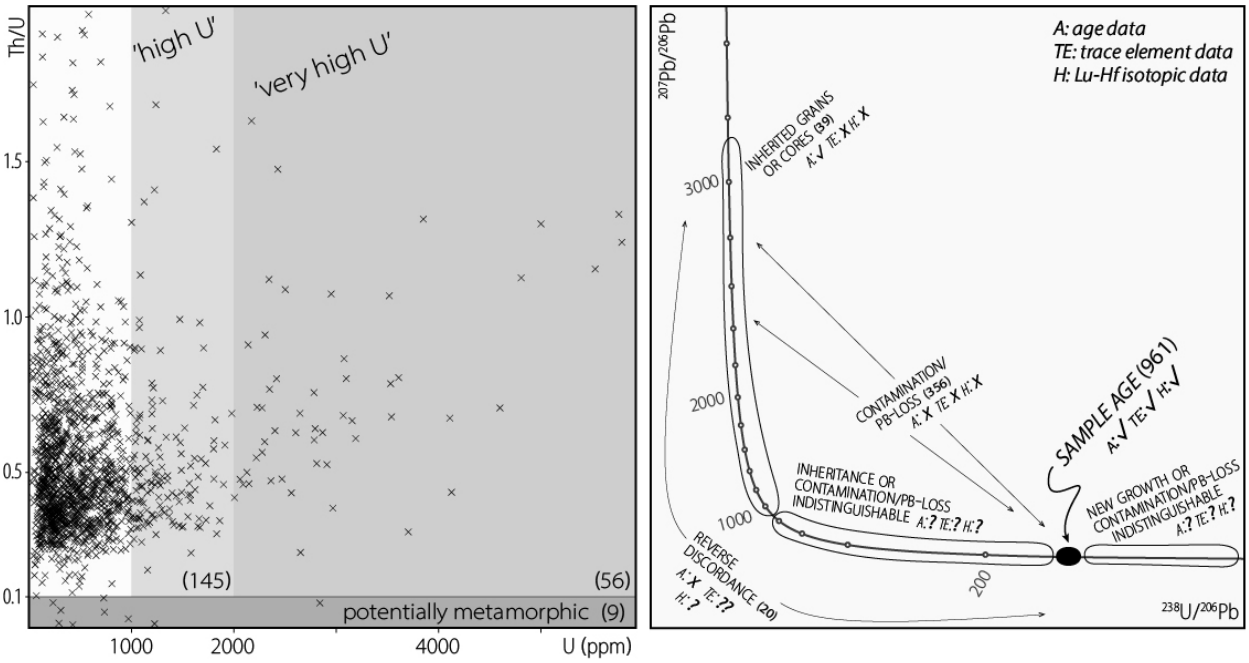

Figure DR2. Filtering schemes for U-Pb age data by zircon U concentrations and Th/U ratios for rock age interpretation (left panel) and by concordia plot relationships for associated zircon TE and Lu-Hf isotope analyses (right panel).

As this study analyzed zircons from igneous rocks for U-Pb ages, TE, and Hf isotopes to reconstruct the geochemical record of arc activity over 150 my, concordia plot relationships can be used to further filter TE data and Hf isotopic analyses prior to plotting and interpretation (Figs. 2, 3 in the accompanying paper) to ensure that these data reflect magma chemistries at the corresponding sample age.

For analyzed zircon populations from igneous rocks that have not experienced significant isotopic perturbations, concordant grains will form a cluster about the main sample age along the concordia curve. For Mesozoic samples, this will lie on the flat part on the right side of the concordia curve (Fig. DR2). TE and Hf isotope data for such analyses may be interpreted as reflecting the compositions of zircon grown within the sample age uncertainty and that the grain age or interpreted sample age can be used with confidence to correct the Hf isotopic data to initial compositions.

Analyses of old (>950 Ma) inherited zircon grains or cores of grains will plot on the steep part on the left of the concordia curve (Fig. DR2). The associated TE and Hf data for zircon inherited analyses older than 950 Ma with discordance between -10% to 20% likely reflect the compositions of zircon crystallized at the analyzed grain age but are not related to the Mesozoic arc activity which is the focus of this study.

Analyses of grains that have experienced Pb-loss or analyses that ablated across old inherited domains and younger domains will plot along lines between the inherited component age and the timing of Pb-loss or younger zircon growth. Mixing of domains with varied ages is herein referred to as contamination. Such analyses cannot be assigned a reliable age for correcting initial isotopic compositions and the TE data cannot be reliably related to magmatism at either the grain age or corresponding sample age.

For analyses younger than 950 Ma that lie along the concordia curve but are not part of the of the main sample age cluster, whether younger or older, interpretation of spot ages is equivocal (Fig. DR2). Inheritance, contamination, or Pb-loss (or other isotopic perturbations) for analyses younger than 950 Ma is difficult to distinguish on concordia plots as these perturbations shift analyses along trajectories parallel and nearly coincident with the concordia curve. For

example, a zircon analysis with a 400 Ma age in a Jurassic sample population with an age of 165 Ma could be possibly interpreted as 1) zircon grain crystallized at 400 Ma; 2) an analysis of a Jurassic rim contaminated by a Paleozoic core crystallized between 400 and 950 Ma; or 3) an inherited 600 Ma grain that has undergone Pb-loss. Thus, the TE data and Hf isotope age correction from such apparently concordant analyses younger than 950 Ma that lie outside of the main sample age cluster will not necessarily reflect zircon grown at those grain ages. Plots of zircon TE and Hf isotopic data (Figs. 2, 3 in the accompanying paper) only include analyses that correspond to concordant U-Pb ages that are part of the main age cluster within their sample population.

TE data were further filtered to exclude analyses that may be affected by microinclusions of glass or accessory minerals which did not significantly perturb the U-Pb systematics of the analyzed volume. TE data were filtered to exclude analyses with high counts of Ca (>2000 counts per second) and P (>10,000 counts per second) as well as high concentrations of Y (>5000 ppm) and LREE ([Ce]>200 ppm; [Pr]>20 ppm ; [Sm]>300 ppm; [Eu]>15 ppm; [Gd]>150 ppm). The above cutoff values are somewhat arbitrary and should depend on the dataset. These choices were guided by comparison to the zircon trace element compilation of Grimes et al. (2015).

REFERENCES CITED ONLY IN THIS DATA REPOSITORY ITEM

Blichert-Toft, J., 2008, The Hf isotopic composition of zircon reference material 91500: Chemical Geology, v. 253, p. 252-257, doi: 10.1016/j.chemgeo.2008.05.014.

Chu, N.C., Taylor, R.N., Chavagnac, V., Nesbitt, R.W., Boella, R.M., Milton, J.A., German, C.R., Bayon, G., and Burton, K., 2002, Hf isotope ratio analysis using multi-collector inductively coupled plasma mass spectrometry: an evaluation of isobaric interference

corrections: Journal of Analytical Atomic Spectrometry, v. 17, p. 1567-1574, doi: 10.1039/b206707b.

Cottle, J.M., Kylander-Clark, A.R.C., and Vrijmoed, J.C., 2012, U-Th/Pb geochronology of detrital zircon and monazite by single shot laser ablation inductively coupled plasma mass spectrometry (SS-LA-ICPMS): Chemical Geology, v. 332-333, p. 136-147.

Cottle, J.M., Burrows, A.J., Kylander-Clark, A.R.C, Freedman, P.A. and Cohen, R.S., 2013, Enhanced sensitivity in laser ablation multi-collector inductively coupled plasma mass spectrometry: Journal of Analytical Atomic Spectrometry, v. 28, p. 1700-1706.

Fisher, C.M., Hanchar, J.M., Samson, S.D., Dhuime, B., Blichert-Toft, J., Vervoort, J.D., and Lam, R., 2011, Synthetic zircon doped with hafnium and rare earth elements: A reference material for in situ hafnium isotope analysis: Chemical Geology, v. 286, p. 32-47.

Hoffman, E.L., 1992, Instrumental Neutron Activation in Geoanalysis: Journal of Geochemical Exploration, v. 44, p. 297-319.

Jackson, S.E., Pearson, N.J., Griffin, W.L., and Belousova, E.A., 2004, The application of laser ablation-inductively coupled plasma-mass spectrometry to in situ U-Pb zircon geochronology: Chemical Geology, v. 211, p. 47-69, doi: 10.1016/j.chemgeo.2004.06.017.

Jochum, K.P., Nohl, U., Herwig, K., Lammel, E., Stoll, B., and Hofmann, A.W., 2005, GeoReM: a new geochemical database for reference materials and isotopic standards: Geostandards and Geoanalytical Research, v. 29, p. 333-338.

Johnson, D.M., Hooper, P.R., and Conrey R.M, 1999, XRF Analysis of Rocks and Minerals for Major and Trace Elements on a Single Low Dilution Li-tetraborate Fused Bead: Advances in X-Ray analysis, v. 41, p. 843-867.

Lackey, J.S., Cecil, M.R., Windham, C.J., Frazer, R.E., Bindeman, I.N., and Gehrels, G.E., 2012, The Fine Gold Intrusive Suite: The roles of basement terranes and magma source development in the Early Cretaceous Sierra Nevada batholith: Geosphere, v. 8, n. 2, p. 292-313, doi: 10.1130/GES00745.1.

Liu, Y., Hu, Z., Zong, K., Gao, C., Gao, S., Xu, J., and Chen, H., 2010, Reappraisement and refinement of zircon U-Pb isotope and trace element analyses by LA-ICP-MS: Chinese Science Bulletin, v. 55, p. 1535-1546, doi: 10.1007/s11434-010-3052-4.

Morel, M.L.A, Nebel, O., Nebel-Jacobsen, Y.J., Miller, J.S., and Vroon, P.Z., 2008, Hafnium isotope characterization of the GJ-1 zircon reference material by solution and laser-ablation MC-ICPMS: Chemical Geology, v. 255 , p. 231-235.

Patchett, P.J., and Tatsumoto, M., 1980, Hafnium isotope variations in oceanic basalts: Geophysical Research Letters, v. 7, p. 1077-1080, doi: 10.1029/GL007i012p01077.

Patchett, P.J., and Tatsumoto, M., 1981, A routine high-precision method for Lu-Hf isotope geochemistry and chronology: Contributions to Mineralogy and Petrology, v. 75, p. 263-267, doi: 10.1007/BF01166766.

Paton, C., Hellstrom, J., Paul, B., Woodhead, J., and Hergt, J., 2011, Iolite: Freeware for the visualisation and processing of mass spectrometric data: Journal of Analytical Atomic Spectrometry, v. 26, p. 2508, doi: 10.1039/c1ja10172b.

Poletti, J.E., Cottle, J.M., Hagen-Peter, G.A., and Lackey, J.S., 2016, Petrochronological constraints on the origin of the Mountain Pass ultrapotassic and carbonatite intrusive suite, California: Journal of Petrology, v. 57, n. 8, doi: 10.1093/petrology/egw050.

Scherer, E.E., Münker, C., and Mezger, K., 2001, Calibration of the lutetium-hafnium clock: Science, v. 293, p. 683-687.

Scherer, E.E., Mezger, K., and Münker, C., 2003, The 176 Lu decay constant discrepancy: Terrestrial samples vs. meteorites: Meteoritics and Planetary Science, v. 38, A136.

Sláma, J., Košler, J., Condon, D.J., Crowley, J.L., Gerdes, A., Hanchar, J.M., Horstwood, M.S.A., Morris, G.A., Nasdala, L., Norberg, N., Schaltegger, U., Schoene, B., Tubrett, M.N., and Whitehouse, M.J., 2008, Plešovice zircon — A new natural reference material for U-Pb and Hf isotopic microanalysis: Chemical Geology, v. 249, p. 1-35, doi: 10.1016/j.chemgeo.2007.11.005.

Söderlund, U., Patchett, P.J., Vervoort, J.D., and Isachsen, C.E., 2004, The 176 Lu decay constant determined by Lu-Hf and U-Pb isotope systematics of Precambrian mafic intrusions: Earth and Planetary Science Letters, v. 219, p. 311-324.

Spencer, K.J., Hacker, B.R., Kylander-Clark, A.R.C., Andersen, T.B., Cottle, J.M., Stearns, M.A., Poletti, J.E., and Seward, G.G.E., 2013, Campaign-style titanite U–Pb dating by laserablation ICP: Implications for crustal flow, phase transformations and titanite closure: Chemical Geology, v. 341, p. 84-101.

Thirlwall, M.F., and Anczkiewicz, R., 2004, Multidynamic isotope ratio analysis using MC-ICP-MS and the causes of secular drift in Hf, Nd and Pb isotope ratios: International Journal of Mass Spectrometry, v. 235, p. 59-81, doi: 10.1016/j.ijms.2004.04.002.

Wiedenbeck, M., Alle, P., Corfu, F., Griffin, W.L., Meier, M., Oberli, F., Quadt, A.V., Roddick, J.C., and Spiegel, W., 1995, Three natural zircon standards for U-Th-Pb, Lu-Hf, trace element and REE analyses: Geostandards and Geoanalytical Research, v. 19, p. 1-23, doi: 10.1111/j.1751-908X.1995.tb00147.x.

Wiedenbeck, M., Hanchar, J. M., Peck, W.H., Sylvester, P., Valley, J., Whitehouse, M., Kronz, A., Morishita, Y., Nasdala, L., Fiebig, J., Franchi, I., Girard, J., Greenwood, R., Hinton, R.,

Kita, N., Mason, P., Norman, M., Ogasawara, M., Piccoli, P., Rhede, D., Satoh, H., Schulz-Dobrick, B., Skår, O., Spicuzza, M., Terada, K., Tindle, A., Togashi, S., Vennemann, T., Xie, Q., and Zheng, Y., 2004, Further Characterization of the 91500 Zircon Crystal: Geostandards and Geoanalytical Research, v. 28, p. 9-39, doi: 10.1111/j.1751-908X.2004.tb01041.x.

Woodhead, J.D., and Hergt, J.M., 2005, A Preliminary Appraisal of Seven Natural Zircon Reference Materials for In Situ Hf Isotope Determination: Geostandards and Geoanalytical Research, v. 29, p. 183-195, doi: 10.1111/j.1751-908X.2005.tb00891.x.